

# A Localization Algorithm for Low-Cost Cleaning Robots Based on Kalman Filter

Zhangjun Song<sup>1,2</sup>, Huifen Liu<sup>1,2</sup>, Jianwei Zhang<sup>3</sup>, Liwei Wang<sup>1,2</sup>, Ying Hu<sup>1,2</sup>

**Abstract**—A novel localization algorithm with low-cost sensors for cleaning robots is presented in this paper, which includes fusing the data of encoders and an electronic compass to estimate the posture state of the robot by using Kalman filter. It judges the confidence of the data of the electronic compass with magnetic field intensity; judges the confidence of data of odometer by the information of slippage and collision. A coverage strategy and map construction methods with the localization algorithm are also introduced. Experimental results show that the proposed algorithm can achieve adequate localization precise enough for complete coverage and the cleaning robots have a superior coverage ratio with the coverage strategy.

**Key words:** **cleaning robots; complete coverage; Kalman filter; localization**

## I. INTRODUCTION

An intelligent cleaning robot is a kind of service robot which is used to clean the floor in indoor environments. More and more intelligent cleaning robots are appearing on the market, such as Roomba ( by iRobot ), CleanMate ( by Infinuvo ), IClebo ( by Yujin Robot ), Koolvac ( by Koolatron ), Trilobite ( by Electrolux ), Hauzen VC-RE72V ( by Samsung ), etc. In order to obtain superior cleaning performance, the robot should have superb pick-up capacity due to a robust brush-roll and suction system. While the robot mostly works on automatic cleaning mode, complete coverage of the room is very important when it is running autonomously. Because of the complicated cleaning environment, it's difficult to cover every unoccupied area. Thus, complete coverage at less time, with less overlapping is the main goal for this kind of product.

Complete coverage for cleaning robots involves the problems of position, navigation and path planning of mobile

robots from an academic point of view. The MIT robot scientists Leonard JJ and Durrant-Whyte HF raised three problems: (1) Where am I? (2) Where am I going? (3) How should I go there? [1] In other words: (1) position and direction in the environment; (2) perception and modeling of the environment; (3) path planning and tracking. For cleaning robots, the first problem is solved by localization with sensors, such as odometer, ultrasound distance sensors, etc. For example, Trilobite ( by Electrolux ) features ultrasound distance sensors and Hauzen VC-RE72V ( by Samsung ) localizes with a MEMS digital gyroscope. The second problem could be solved by a map of the room. The third problem could be solved by a coverage strategy. For example, Roomba cleans the room with outer spiral path planning; Hauzen VC-RE72V runs back and forth in a roundabout way. However, outer spiral path planning would take too much time to achieve complete coverage. Worse is that it cannot achieve complete coverage when there are obstacles in the room. If the robot runs back and forth in a roundabout way, precise localization is necessary. Trilobite and Hauzen VC-RE72V achieve this via expensive sensors. This results in products that are too expensive.

In this paper, we explore complete coverage for cleaning robots with low-cost sensors. A coverage strategy with wall-following and cleaning the central area in a roundabout way is proposed. A localization algorithm that fuses data from encoders and of an electronic compass by using a Kalman filter is described in detail.

## II. KINEMATIC MODEL OF CLEANING ROBOTS

The cleaning robot studied in this paper has a differential drive mobile base which is made of two fixed wheels and a castor wheel, as shown in Fig.1. Each fixed wheel axis contains an encoder, which can detect the speed of the wheel.

The robot posture can be described in terms of the two coordinates  $x$ ,  $y$  of the origin and the orientation angle  $\theta$  [2]. Hence, the robot posture is given by the vector

$$\mathbf{p} = \begin{pmatrix} x \\ y \\ \theta \end{pmatrix} \quad (1)$$

With the kinematic model of differential drive mobile robots [3], we get the incremental posture of the robot in a sampling period

$$\Delta x = \Delta s \cos(\theta + \Delta\theta) \quad (2)$$

$$\Delta y = \Delta s \sin(\theta + \Delta\theta) \quad (3)$$

Manuscript received December 13, 2009. This work was supported by Guangdong natural science fund (9478922035-X003357) and Shenzhen basic research plan ( JC200903160379A), CAS Knowledge Innovation Project (KGCXZ-YW-128).

Zhangjun Song is with <sup>1</sup>Shenzhen Institutes of Advanced Technology, Chinese Academy of Sciences and <sup>2</sup>The Chinese University of Hong Kong (e-mail: zj.song@siat.ac.cn).

Huifen Liu is with <sup>1</sup>Shenzhen Institutes of Advanced Technology, Chinese Academy of Sciences and <sup>2</sup>The Chinese University of Hong Kong (e-mail: hf.liu@sub.siat.ac.cn)

Jianwei Zhang, is with <sup>3</sup>the Faculty of University of Hamburg, Germany (e-mail: zhang@informatik.uni-hamburg.de.).

Liwei Wang is with <sup>1</sup>Shenzhen Institutes of Advanced Technology, Chinese Academy of Sciences and <sup>2</sup>The Chinese University of Hong Kong (e-mail: lw.wang@siat.ac.cn)

Ying Hu is with <sup>1</sup>Shenzhen Institutes of Advanced Technology, Chinese Academy of Sciences and <sup>2</sup>The Chinese University of Hong Kong (e-mail: ying.hu@siat.ac.cn)

$$\Delta\theta = \frac{\Delta s_r - \Delta s_l}{b} \quad (4)$$

Where  $(\Delta x \ \Delta y)$  is the distance traveled by the robot in a sampling interval;  $\Delta\theta$  is the angle changed in this period;  $\Delta s_l$ ,  $\Delta s_r$  are the distances traveled by the left wheel and right wheel respectively in this period;  $b$  is the distance between two wheels; and

$$\Delta s = \frac{\Delta s_r + \Delta s_l}{2} \quad (5)$$

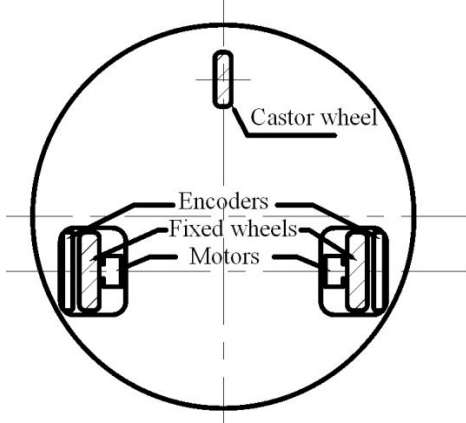


Fig. 1 The differential-drive mobile base of cleaning robots  
Therefore, we get the updated posture of the robot, namely

$$\begin{aligned} \mathbf{p}' &= \begin{pmatrix} x' \\ y' \\ \theta' \end{pmatrix} = \mathbf{p} + \begin{pmatrix} \Delta s \cos(\theta + \Delta\theta) \\ \Delta s \sin(\theta + \Delta\theta) \\ \Delta\theta \end{pmatrix} \\ &= \begin{pmatrix} x \\ y \\ \theta \end{pmatrix} + \begin{pmatrix} \Delta s \cos(\theta + \Delta\theta) \\ \Delta s \sin(\theta + \Delta\theta) \\ \Delta\theta \end{pmatrix} \end{aligned} \quad (6)$$

With function (4) and (5), we get the posture of the robot after the data from the odometer are updated, given by

$$\begin{aligned} \mathbf{p}' &= f(x, y, \theta, \Delta s_r, \Delta s_l) \\ &= \begin{pmatrix} x \\ y \\ \theta \end{pmatrix} + \begin{pmatrix} \frac{\Delta s_r + \Delta s_l}{2} \cos(\theta + \frac{\Delta s_r - \Delta s_l}{b}) \\ \frac{\Delta s_r + \Delta s_l}{2} \sin(\theta + \frac{\Delta s_r - \Delta s_l}{b}) \\ \frac{\Delta s_r - \Delta s_l}{b} \end{pmatrix} \end{aligned} \quad (7)$$

$\Delta s_l$ ,  $\Delta s_r$  can be directly estimated with the data of odometers.

### III. SENSORS OF LOCALIZATION FOR CLEANING ROBOTS

The traditional sensors for mobile robots localization is odometer. Odometry is the most widely used navigation method for mobile robot positioning; it provides good short-term accuracy, is inexpensive, and allows very high sampling rates. However, the fundamental idea of odometry is the integration of incremental motion information over time, which leads inevitably to the unbounded accumulation of errors [4]. Specifically, orientation errors will cause large lateral position errors, which increase proportionally with the distance travelled by the robot [5].

Because of the slippage, collision and some other reasons, the precision of localization does not keep up with the rapid development of mobile robots. Many new sensors are recommended for use in mobile robots for localization, such as infrared sensors, ultrasonic distance sensors, laser ranging sensors, gyroscope, RFID, wireless network sensors, GPS, etc. The cost of these sensors for mobile robots in indoor environments is illustrated in Fig.2.

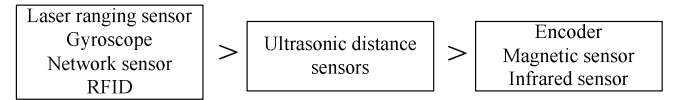


Fig. 2 Cost of sensors for localization

Inertial navigation uses gyroscopes and accelerometers to measure the rate of rotation and acceleration, respectively. Inertial navigation systems have the advantage that they are self-contained, that is, they don't need external references. However, inertial sensor data drift with time because of the need to integrate rate data to yield position; any small constant error increases without bound after integration. Gyroscopes, accelerometers and encoders have the same disadvantage, but encoders are more inexpensive [6].

Sensors which provide a measure of absolute heading are extremely important in solving the navigational requirements of autonomous platforms. The electronic compass is such a sensor.

In our project, in order to obtain a much better positioning accuracy with low cost sensors, we choose encoders and an electronic compass for localization.

### IV. MULTI-INFORMATION FUSION OF THE ELECTRONIC COMPASS AND AN ENCODER-BASED KALMAN FILTER

The most widely used method for sensor fusion in mobile robot applications is the Kalman filter. This filter is often used to combine all measurement data (e.g., for fusing data from different sensors) to get an optimal estimate in a statistical sense. If the system can be described with a linear model and both the system error and the sensor error can be modeled as Gaussian white noise, then the Kalman filter will provide a unique statistically optimal estimate for the fused data. This means that under certain conditions the Kalman filter is able to find the best estimates based on the "correctness" of each individual measurement.

The robot's position and angle could be estimated with encoders, but then an accumulated error could not be avoided. The angle also could be measured with an electronic compass, but the result will be wrong if a disturbance occurs. We fuse

data from encoders and an electronic compass to estimate the posture state of the robot by using a Kalman filter.

#### A. Observation Model

The electronic compass detects the absolute heading of the robot with respect to the magnetic North. As shown in Fig. 3, the 2-axis electronic compass has two magneto-resistive sensors  $S_x$  and  $S_y$ , which are perpendicular to each other. The magnetic North is by direction ON. The azimuth angle of the electronic compass is defined as the angle from ON to OX clockwise, given by  $\psi$ . Given the horizontal component of the earth's magnetic field is  $H_0$ , the magnetic field components detected by magneto-resistive sensors  $S_x$  and  $S_y$  are

$$H_x = H_0 \cos \psi \quad (8)$$

$$H_y = -H_0 \sin \psi \quad (9)$$

From equation (8) and (9), we get

$$\psi = -\arctan\left(\frac{H_y}{H_x}\right) \quad (10)$$

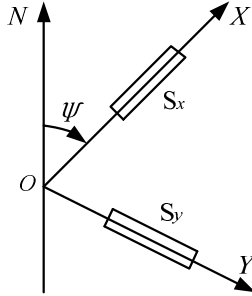


Fig. 3 Schematic diagram of the electronic compass  
The posture of the robot estimated by the electronic compass is

$$Z(k) = \begin{pmatrix} 0 & 0 & 1 \end{pmatrix} \begin{pmatrix} x \\ y \\ \theta \end{pmatrix} + V(k) \quad (11)$$

The observation model of the robot is

$$Z(k) = HX(k) + V(k) \quad (12)$$

Where  $H = \begin{pmatrix} 0 & 0 & 1 \end{pmatrix}$ ,

$$X(k) = \begin{pmatrix} x \\ y \\ \theta \end{pmatrix}, \text{ and } V(k) \text{ is the measurement noise.}$$

#### B. Multi-sensor information fusion based on a Kalman filter

##### (1) State estimation of the orientation angle

The state of the angle at moment  $k$  is estimated by the state at moment  $k-1$  and the control input. The angle at this moment is measured based on the angle at the last moment, with the system model of the Kalman filter, namely

$$X(k|k-1) = A X(k-1|k-1) + B U(k) \quad (13)$$

The angle is estimated by

$$\theta(k|k-1) = \theta(k-1|k-1) + \theta_e(k) \quad (14)$$

Where  $\theta(k|k-1)$  is the angle state at moment  $k$ , which is predicted based the state at moment  $k-1$ ;  $\theta(k-1|k-1)$  is the optimal results at moment  $k-1$ ;  $\theta_e(k)$  is the incremental value of the encoder from moment  $k-1$  to moment  $k$ .

##### (2) The covariance of the angle updated

After we have estimated the angle, we update the covariance by

$$P(k|k-1) = A P(k-1|k-1) A' + Q \quad (15)$$

Where  $Q$  is the covariance of the system process. In this measuring system for the angle, the key factor which decides the magnitude of  $Q$  is the precision of the relative displacement measured by the encoder in a sampling period. The error of the relative displacement measured by the encoder is caused by slippage or collision, which could be detected by bumper sensors in the front of the robot and the encoder installed on the castor wheel. Thereby we get

$$Q(k) = f(\text{collide\_sensor}(k), \text{front\_ring}(k)) \quad (16)$$

Where  $\text{collide\_sensor}(k)$  is the state of collision at moment  $k$  detected by the bumper sensors;  $\text{front\_ring}(k)$  is a function, which is decided by the encoder value installed in the castor wheel and the value of the encoders installed in the fixed wheels. The state covariance of the angle is predicted by

$$P(k|k-1) = P(k-1|k-1) + f(\text{collide\_sensor}(k), \text{front\_ring}(k)) \quad (17)$$

##### (3) Calculating the optical estimate value of the state based on Kalman filter gain

After the angle state is estimated, the angle measured by the electronic compass is also collected. After fusing the predicted angle and the angel measured by the electronic compass, we obtain the optical estimate value of the state at this moment, given by

$$\begin{aligned} \theta(k|k) &= \theta(k|k-1) + \\ &Kg(k)(\theta_e(k) - \theta(k|k-1)) \end{aligned} \quad (18)$$

Where  $Kg$  is the Kalman Gain. It can be obtained from

$$Kg(k) = P(k|k-1) / (P(k|k-1) + R) \quad (19)$$

Where  $P(k|k-1)$  is angle covariance at moment  $k$ , obtained from function (17);  $R$  is the covariance of the measurement noise. For the electronic compass, the key factor which decides the measurement noise is the magnetic field intensity. The measurement noise changes with the change of magnetic field intensity. We assume that the relations between measurement noise and magnetic field intensity can be given by  $R(k) = f(m(k))$ , where  $m(k)$  is the magnetic field intensity at moment  $k$ .

Therefore the Kalman Gain can be calculated by

$$Kg(k) = P(k|k-1)/(P(k|k-1) + f(m(k))) \quad (20)$$

(4) Covariance matrix updated

In order to make the Kalman filter work continuously, we need not only calculate the optimal estimate value of angle  $\theta(k|k)$  at moment  $k$ , but also calculate the covariance of  $\theta(k|k)$  at moment  $k$ . It can be obtained by

$$P(k|k) = (1 - Kg(k))P(k|k-1) \quad (21)$$

When the system goes into  $k+1$  state,  $P(k|k)$  will substitute  $P(k|k-1)$  by equation (21). In this way, the Kalman filter will work continuously. The flow of the Kalman filter is shown in Fig. 4.

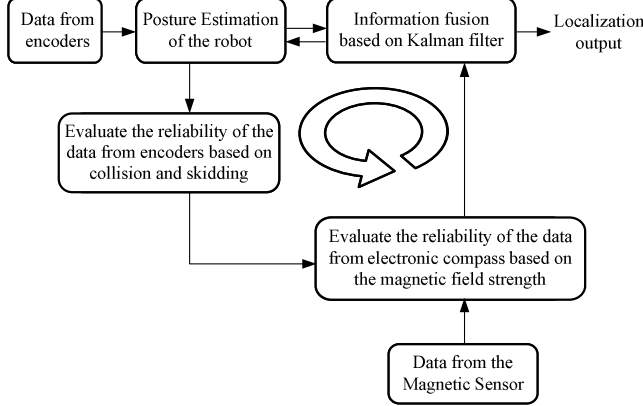


Fig. 4 Flow of the Kalman filter

## V. COVERAGE STRATEGY AND MAP CONSTRUCTION

### A. Coverage strategy

The coverage strategy is proposed as followings:

The robot begins to clean at any point in the room. It runs directly until it is blocked, then it begins the wall following algorithm. It constructs the map while cleaning, choosing the starting point as the coordinate origin. If the robot has found the charger when cleaning while following the wall, the robot sets a new coordinate, whose coordinate origin is chosen at the point where the charger is located. If it has not found the charger when it follows the wall, the coordinate is not changed. The boundary of the room will be completely marked in the map when the cleaning while following the wall is over [7-8]. After this step, the robot goes back to the coordinate origin and begins to clean the central area of the room in a roundabout way. If there is an obstacle ahead, it stops and then runs in the opposite direction, which is parallel to the original path. The distance between the two parallel paths is a step, which could be adjusted based on the width of the brush. The path planning in the centre area of the room is proposed in Fig. 5. If the robot gets short of power when it is cleaning the centre area of the room, it records this position and goes to the charger to automatically recharge, then returns to that position and continues to clean when recharging is over [9]. All the traces of the robot will be recorded in the map. When too many traces of the robot overlap the boundary of the room, we suppose that the robot has got to the other side of the room compared to the side where the charger is. Because of the obstacles, one or two

margins may be missed, which can be analyzed from the maps. The last step is to find the margin and clean this area. After that, the cleaning of the whole room is over. The coverage strategy is shown in Fig. 6

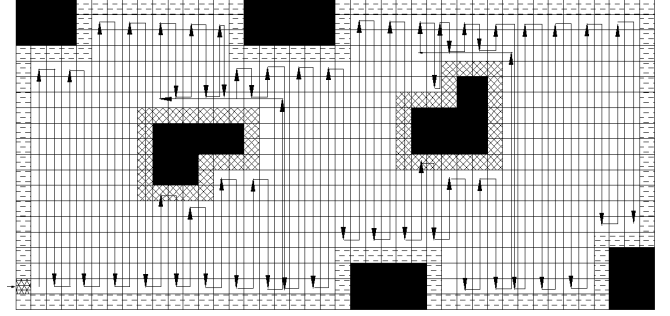


Fig. 5 Path planning when the robot cleans the central area of the room

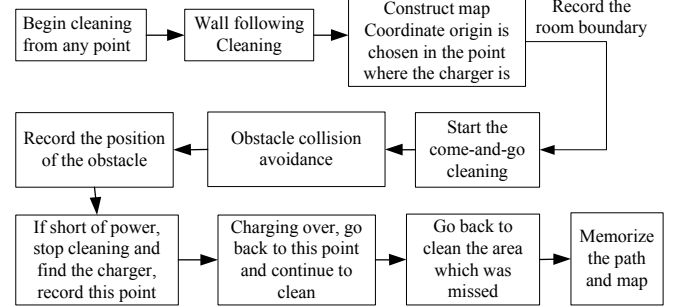


Fig. 6 Coverage strategy of the cleaning robot

### B. Map construction and recording

In the map, the coordinate origin is chosen at the point where the charger is or the starting point, and the Y-axis is set along one side of the room. When the robot is cleaning, the trace of the robot and the coordinates of the points where a collision happens are recorded in the memory. With such information, the map is constructed. The map can be displayed on the screen if the robot links to a computer via wireless communication module. The path of the robot and the profile of the obstacles are demonstrated in real-time.

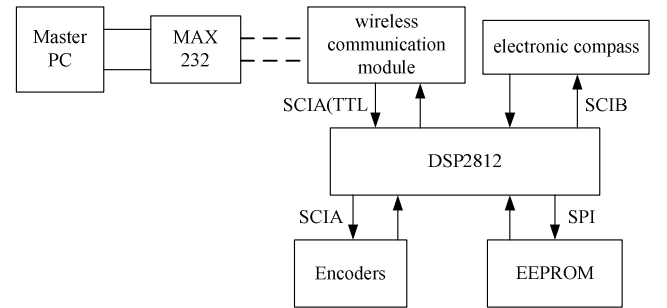


Fig. 7 Schematic diagram of the circuit for recording

The map is also recorded in EEPROM. Therefore, the map information will not be lost even when the robot is turned off. The schematic diagram of the hardware circuit for map recording is shown in Fig. 7.

## VI. EXPERIMENTS

### 1) Wall following

In order to verify the efficiency of the fusion based on a Kalman filter, cleaning while following the wall is tested in the same example of workspace, as shown in Fig. 8. The size

of the workspace is 4380mm\*3850mm. There is a desk and some chairs with legs of steel in the room. Linear displacement is measured by the encoders. Angular displacement is estimated with the information from the encoders and/or the electronic compass. The trace of the robot in the map is shown in Fig. 9, which is localized only with the information from the encoders. In Fig. 10, linear displacement is measured by the encoders, while angular displacement is estimated with the information from the electronic compass. In Fig. 11, linear displacement is measured by the encoders, while angular displacement is estimated with the information from the encoders and the electronic compass based on a Kalman filter.

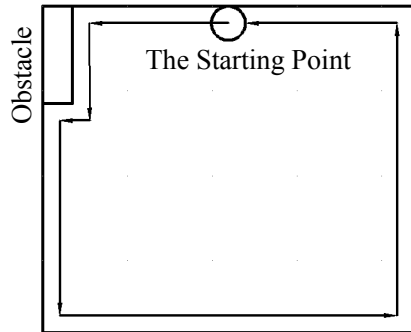


Fig. 8 Environment of the localization experiments

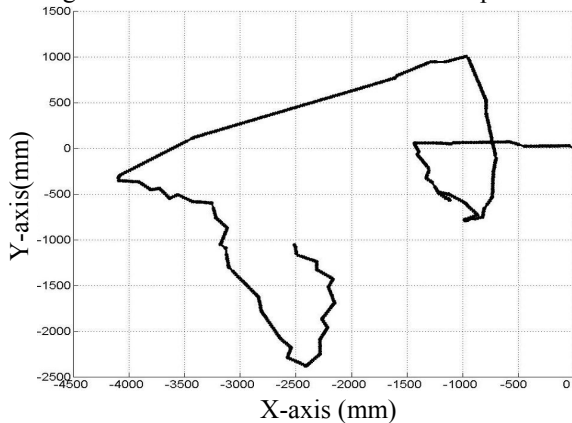


Fig. 9 Trace of the robot only with the information from the encoders

As shown in Fig.9, we can see that the angle estimated only with the information from the encoders has obviously accumulated an error. If there is something wrong with the angle estimation in some sampling period, the result is disastrous. The robot may lose its way after a certain number of turns.

As shown in Fig.10, the angle estimated only with information from the electronic compass is much better, for it has no accumulated error. Although most of the time the estimated angle is right, it is sometimes wrong. After analyzing the data from the electronic compass, we find that the magnetic field intensity is very weaker or stronger when this happens. The earth's magnetic field is relatively stable, however, when there are iron or steel appliances like refrigerators on the surface of the earth at some points, the magnetic field intensity at this point may changes and is different from that at other points.

From Fig.9 to Fig. 11, it can be seen that the trace of the robot in Fig.11 is mostly similar to a rectangular shape, namely the real profile of the room. Thereby we can conclude that the information from encoders and an electronic compass based on a Kalman filter yields higher localization accuracy than that of only encoders or only an electronic compass.

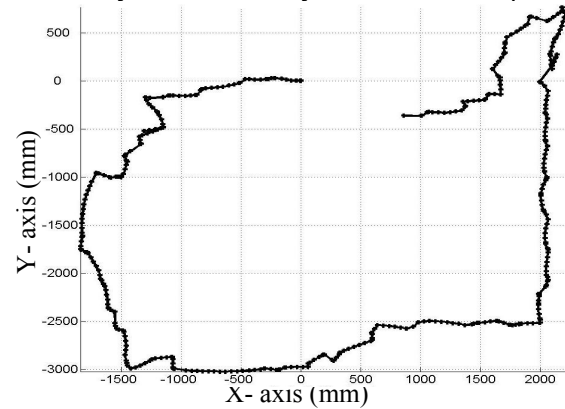


Fig. 10 Trace of the robot (linear displacement was measured by the encoders, angular displacement was estimated with the information from the electronic compass)

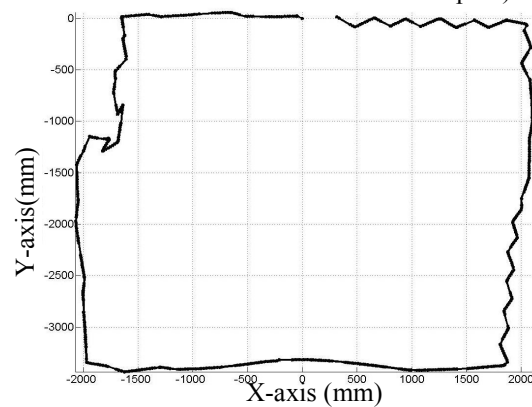


Fig. 11 Trace of the robot (linear displacement was measured by the encoders, while angular was estimated with the information from the encoders and the electronic compass based on a Kalman filter)

## 2) Localization accuracy

The experiments are carried out in a 10m<sup>2</sup> rectangular workspace, with an obstacle in the centre. When the robot stops or turns at any point, this point is marked on the floor, as shown in Fig. 12. Connecting the marked points, we get the real path of the robot. We add the real path of the robot into the map, as shown in Fig. 13. In Fig. 13, the red line is the real path; the blue line is the path in the map, which is calculated by the position information after fusion. It can be seen that the positioning error in the X-axis and Y-axis direction is less than 0.5m.



Fig. 12 Precise experiments

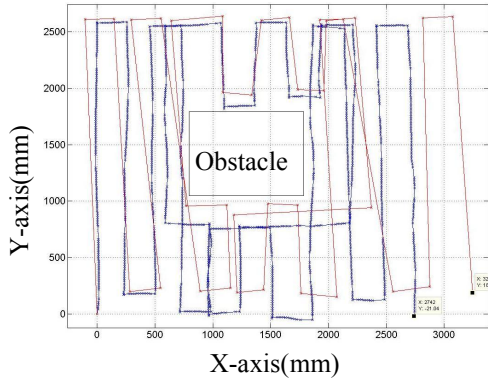


Fig. 13 Positioning error in the map

### 3) Path planning and map construction

In order to verify the efficiency of the coverage algorithm, we explore the coverage ratio by experiments in the same workspace. Experiments are carried out in a  $3.75 \times 4.5 \text{ m}^2$  room, where a  $0.75 \times 0.5 \text{ m}^2$  obstacle is located near the side, and two  $0.6 \times 0.4 \text{ m}^2$  obstacles are in the centre. The map after cleaning is shown in Fig. 14. The red grid signifies that this area is occupied by obstacles and the blue grid signifies that this area is cleaned without collision.

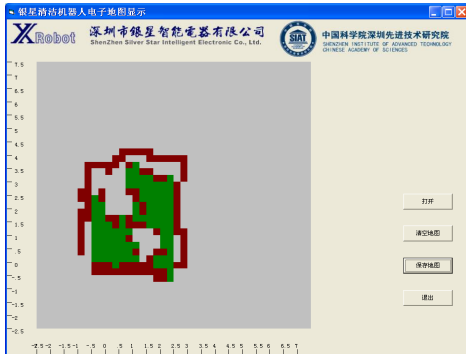


Fig. 14 The map after cleaning

Table 1 Experimental results

	Total grids	Red grids	Green grids	Blank grids	Un-cleaned grids	Coverage ratio
1	270	91	138	27	13	95.2%
2	270	88	145	37	23	91.5%
3	270	89	148	33	19	93.0%
4	270	93	146	31	17	93.7%
5	270	98	135	37	23	91.5%
6	270	92	143	35	21	92.2%
7	270	84	150	36	22	91.9%
8	270	104	137	29	15	94.4%
9	270	102	139	29	15	94.4%
10	270	93	145	32	18	93.3%

In these experiments, each grid represents an area of  $0.25 \times 0.25 \text{ m}^2$ . All the areas of the room have 270 grids, of which the obstacles occupy 27 grids. The robot cleaned the same room ten times with the coverage algorithm proposed in section V. The experimental results are shown in Table 1.

From Table 1 it can be seen that the coverage ratio (ratio of the cleaned area to the total area) with the proposed coverage algorithm is over 90%. The electronic map with grids can express the cleaned area and the area occupied with obstacles effectively.

## VII. CONCLUSION

In this paper, a novel localization algorithm with low-cost sensors is presented for cleaning robots. It fuses data from encoders and an electronic compass to estimate the posture state of the robot by using a Kalman filter. The algorithm provides an adequately precise localization for complete coverage by judging the confidence of the electronic compass with magnetic field intensity. With the proposed coverage strategy, the robot can clean the room with more than a 90% coverage ratio, which is encouraging. However, the disturbance of the electronic compass from iron or steel appliances like refrigerators is still a problem.

## ACKNOWLEDGMENT

The authors would like to thank Shenzhen Silver Star Intelligent Electronic Co., Ltd for providing cleaning robots to test. We also thank Yingjie Zhang from the Shenzhen Institute of Advanced Integration Technology, Chinese Academy of Sciences/The Chinese University of Hong Kong, for his contribution to experiments.

## REFERENCES

- [1] Leonard J J, Durrant-Whyte H F. Mobile robot localization by tracking geometric beacons. *IEEE Transactions on Robotics and Automation*, 1991,7(3): 376-382
- [2] Canudas de Wit C, Siciliano B, Bastin G. *Theory of Robot Control*. New York: Springer, 2001. 265-306
- [3] Hamidreza C, Steven M. La Valle. Minimum wheel-rotation paths for differential drive mobile robots among piecewise smooth obstacles. *International Conference on Robots and Automation*, 2007. Roma, Italy, 10-14 April pp.2718 -2723
- [4] Borenstein J, Feng L. Measurement and Correction of Systematic Odometry Errors in Mobile Robots. *IEEE Transactions on Robotics and Automation* (S1042-296X), 1996, 12(6): 869-880
- [5] J.Borenstein, H. R. Everett and L. Feng, "Sensors and Methods for Mobile Robot Positioning", 1996 new ed. J.Borenstein, Ed. The University of Michigan, 1996, pp. 95-109
- [6] Borenstein. J, Everett. H. R, Feng. L, et al. Mobile robot Positioning sensors and techniques. *Journal of Robotic Systems*, 1997,14(4): 231-249
- [7] J. L. Diaz, S. Leon, J. H. Sossa. Automatic path planning for a mobile robot among obstacles of arbitrary shape. *IEEE Transactions on Systems, Man, and Cybernetics-Part B: Cybernetics*. 1999(28): 467-472
- [8] Julier S J, Uhlmann J K, Durrant-Whyte H F. A new approach for the nonlinear transformation of mean and covariances in filters and estimators. *IEEE Transactions on Automatic Control*, 2000, 45(3): 477-482
- [9] Zhang C G, Xi Y G Robot rolling path planning based on locally detected information. *Acta Automatica Sinica*, 2003, 29(1): 38-44.